Available online at www.sciencedirect.com
ScienceDirect
Thin Solid Films 516 (2008) 1359–1364
www.elsevier.com/locate/tsf

Some studies on highly transparent wide band gap indium molybdenum oxide thin films rf sputtered at room temperature

E. Elangovan [a,*], A. Marques [a], A.S. Viana [b], R. Martins [a], E. Fortunato [a]

[a] Materials Science Department, CENIMAT/I3N and CEMOP-UNINOVA, FCT-UNL, Campus de Caparica, 2829-516 Caparica, Portugal
[b] Faculty of Sciences, University of Lisbon, SPM Laboratory, Ed.ICAT, Campo Grande, Lisbon, 1749-016, Portugal

Available online 5 April 2007

Abstract

Transparent wide band gap indium molybdenum oxide (IMO) thin films were rf sputtered on glass substrates at room temperature. The films were studied as a function of sputtering power (ranging 40–180 W) and sputtering time (ranging 2.5–20 min). The film thickness was varied in the range 50–400 nm. The as-deposited films were characterized by their structural (XRD), morphological (AFM), electrical (Hall Effect measurements) and optical (visible-NIR spectroscopy) properties. XRD studies revealed that the films are amorphous for the sputtering power ≤ 100 W and the deposition time ≤ 5 min, and the rest are polycrystalline with a strong reflection from (222) plane showing a preferential orientation. A minimum bulk resistivity of 2.65×10^{-3} Ω cm and a maximum carrier concentration of 4.16×10^{20} cm^{-3} are obtained for the crystalline films sputtered at 180 W (10 min). Whereas a maximum mobility (19.5 $cm^2\ V^{-1}\ s^{-1}$) and average visible transmittance ($\sim 85\%$) are obtained for the amorphous films sputtered at 80 W and 100 W respectively for 10 min. A minimum transmittance ($\sim 18\%$) was obtained for the crystalline films sputtered at 180 W (~ 305 nm thick). The optical band gap was found varying between 3.75 and 3.90 eV for various sputtering parameters. The obtained results are analyzed and corroborated with the structure of the films.

Keywords: Transparent conducting oxides; Sputtering; Indium molybdenum oxide; Room temperature; Structural properties

1. Introduction

A recent development on the wide band gap oxide semiconductors promoted the transparent electronics as one of the most advanced topics [1]. The deviation of oxygen stoichiometry classifies these semiconductors either as a passive element (such as LCDs, OLEDs, solar cells, photo-catalytic purification, optical and gas sensors, etc.) or an active element (such as TFTs, LEDs, lasers, UV sensors etc.) [1,2]. Wide band gap n-type semiconductors such as In_2O_3, ZnO and TiO_2 that do not undergo decomposition upon irradiation or heating are useful in dye sensitized applications [2]. Recently wide band gap semiconductor nanowires have fascinated the researchers globally [3]. The wide band gap semiconductor materials require high carrier concentration in order to reach an optical gain that is high enough for lasing action [4]. Recently, a novel indium molybdenum oxide (IMO) films were reported by Meng et al. [5] with high carrier concentration and wide band gap. Further, IMO has high mobility with less impurity [5] which is a criterion needed to exploit transparent electronics. A detailed literature survey revealed that there is a clear paucity of reports on room temperature (RT) processing of IMO films, especially utilizing sputtering technique. In this context, we have demonstrated in our preliminary work [6] that minimum O_2 vol.% (3.5%) is one of the effective parameters to achieve better IMO films by rf sputtering at RT. In order to improve the conductivity, the films reported in the present study were sputtered with various deposition time and sputtering power. With the best of authors' knowledge the IMO films rf sputtered at room temperature is reported for the first time from our group.

2. Experimental details

The films were sputtered from an In_2O_3 (95 wt.%): Mo (5 wt.%) target (2″ diameter) on glass substrates ($100\times100\times1$ mm^3) at room temperature with different sputtering power (ranging 40–180 W) and sputtering time (2.5–20.0 min). Partial

* Corresponding author. Tel.: +351 212948562 (#11609); fax: +351 21294 8558.
E-mail addresses: elankam29@yahoo.com, elam@fct.unl.pt (E. Elangovan).

0040-6090/$ - see front matter © 2007 Elsevier B.V. All rights reserved.
doi:10.1016/j.tsf.2007.03.155

Table 1
Various properties of IMO films as a function of sputtering power and sputtering time

Parameter	Thickness (nm)	AVT (%)	E_g (eV)	ρ (Ω cm)	μ (cm^2/Vs)	N (cm^{-3})
At constant sputtering time of 10 min						
40 W	54	80.9	3.86	$>10^4$	–	–
60 W	90	73.0	3.84	$>10^4$	–	–
80 W	138	79.4	3.82	1.95×10^{-2}	19.5	1.64×10^{19}
100 W	157	85.3	3.80	1.49×10^{2}	2.9	1.44×10^{16}
120 W	206	83.0	3.77	3.90×10^{-2}	8.6	1.86×10^{19}
140 W	239	77.1	3.80	1.11×10^{-2}	10.5	5.39×10^{19}
160 W	261	64.8	3.84	5.15×10^{-3}	9.1	1.33×10^{20}
180 W	305	17.7	3.75	2.65×10^{-3}	5.7	4.16×10^{20}
At constant sputtering power of 120 W						
2.5 min	56	78.0	3.84	3.24×10^{-3}	7.0	2.76×10^{20}
5.0 min	102	72.8	3.83	2.08×10^{-3}	18.4	1.63×10^{20}
7.5 min	156	83.9	3.80	1.90×10^{-2}	10.4	3.04×10^{19}
10.0 min	206	83.0	3.77	3.90×10^{-2}	8.6	1.86×10^{19}
12.5 min	253	76.3	3.80	7.32×10^{-3}	15.5	5.49×10^{19}
15.0 min	300	71.8	3.80	4.24×10^{-3}	13.6	1.08×10^{20}
17.5 min	357	71.0	3.88	6.48×10^{-3}	8.7	1.10×10^{20}
20.0 min	398	72.3	3.90	5.23×10^{-3}	13.7	8.70×10^{19}

AVT — Average visible transmittance; E_g — band gap; ρ — bulk resistivity; μ — mobility; N — carrier concentration.

pressures of oxygen (0.5 sccm) and argon (30.0 sccm) were maintained at $\sim1.1\times10^{-3}$ and $\sim3.0\times10^{-1}$ Pa respectively, and the sputtering pressure at $\sim6.0\times10^{-1}$ Pa. The details on the other parameters can be found in our previous study on these films [6]. The sputtered films were characterized for their structural, morphological, electrical and optical properties. A radio frequency power generator (13.6 MHz) from Advanced Energy (Model: RFX 2500) was used for sputtering the target. The crystal structure of the films was confirmed using an X-ray diffractometer (DMAX-III C from Rigaku; sealed tube, Cu K_α radiation) in Bragg–Brentano geometry ($\theta/2\theta$ coupled). The film thickness was measured using a stylus profilometry (Solan Dektak 3D) with an accuracy of ±20 nm. The electrical parameters were measured using a Hall measurements setup (Bio-Rad HL5500 Hall system) with a permanent magnet of 5 kG. Optical transmittance (T) was measured using a double beam spectrophotometer (Shimadzu UV-3100). Tapping mode AFM experiments were performed in a Multimode AFM microscope coupled to a Nanoscope IIIa Controller (Digital Instruments, Veeco). Commercially etched silicon tips with typical resonance frequency of ca. 300 kHz were used as AFM probes.

3. Results and discussion

The IMO films were studied as a function of sputtering power (40–180 W) and sputtering time (2.5–20 min). The film thickness measured at various places were found to be uniform, and the average value was found ranging ~50 to 300 nm for the variation in sputtering power from 40 to 180 W, and ranging ~50 to 400 nm for the variation in sputtering time from 2.5 to 20.0 min (Table 1). This confirms that the deposition rate was increased with the increasing sputtering power, and was

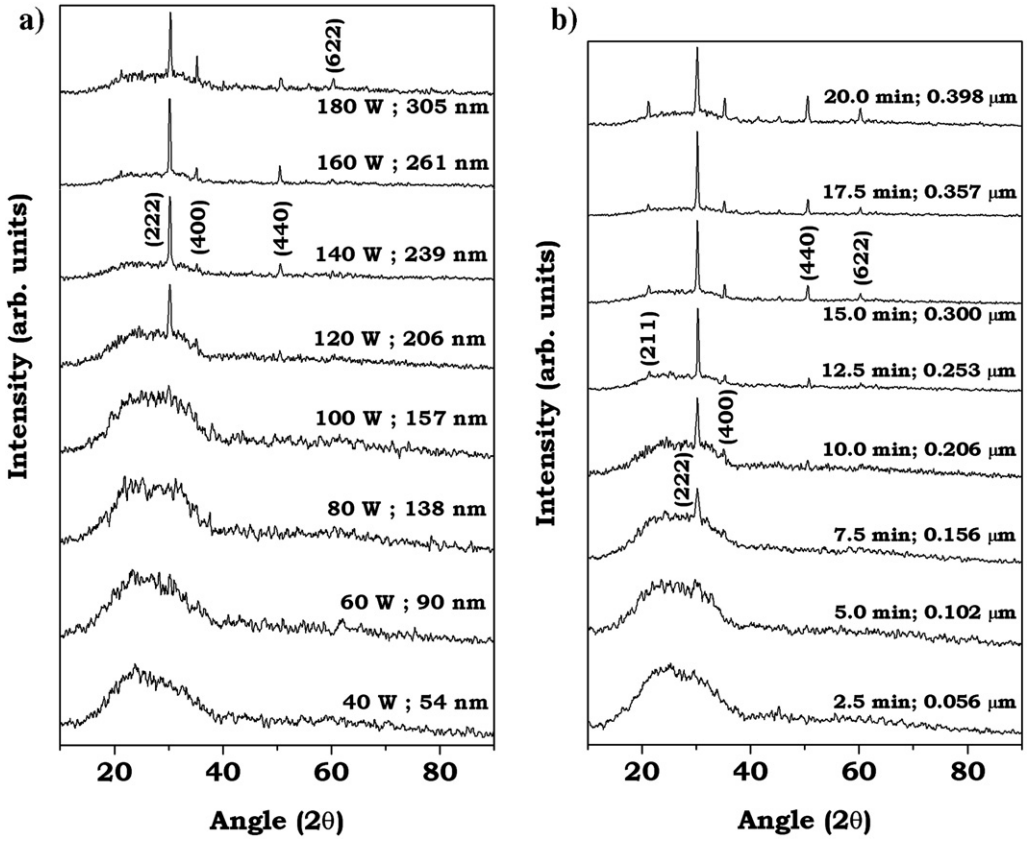

Fig. 1. XRD patterns of thickness dependent IMO films: (a) as a function of sputtering power (10 min) and (b) as a function of sputtering time (120 W).

constant for the various sputtering time. The films sputtered at 120 W showed a tendency to crystallize and thus the consecutive depositions were made by sputtering with different sputtering time at 120 W and the results are described below.

3.1. Structural studies

The typical XRD patterns (2θ ranging 10–90°) are shown as a function of sputtering power for 10 min (Fig. 1a) and sputtering time at 120 W (Fig. 1b). It is perceptible (Fig. 1a) that the films sputtered with ≤100 W (≤160 nm thick) show a broad hump (20–40°) which is the characteristic of an amorphous structure. The crystallization commences when the sputtering power is increased above 100 W. This probably indicates that the sputtered species are acquiring more thermal energy and diffuse over the substrate surface to occupy proper lattice positions. The reflections obtained from (211), (222), (400), (440) and (622) planes were identified by matching with those of cubic bixbyite In_2O_3 (ICDD file number: 06-0416). The strongest reflection from (222) plane is showing a preferential orientation. The intensity of the (222) reflection increases with increasing sputtering power until 160 W but then decreases. The amorphous hump observed for the films sputtered at ≤100 W (≤160 nm thick) decreases with increasing sputtering power and normalizes at 160 W (~261 nm thick). A very weak reflection along (622) plane was observed at 180 W. Fig. 1b shows the films are amorphous for the sputtering time ≤5 min (≤100 nm thick). A well distinguished reflection is obtained from (222) plane for the films sputtered for 7.5 min. The intensity of this reflection increases with increasing sputtering time and suffocate the amorphous hump. Other reflections from the planes such as (400), (440) and (622) were observed as shown in Fig. 1b. An additional reflection from (211) plane is observed for the sputtering time above 10.0 min.

The foregoing discussion suggests that the variation of both the sputtering power and sputtering time are the effective parameters to control the structure of IMO films. Although the variation of these parameters is directly related with film thickness which is a material property, it is not straightforward to ascribe the change in structural properties to thickness for the following reasons. It is perceptible that the films sputtered at 100 W for 10 min and those sputtered at 120 W for 7.5 min have same thickness values (157 and 156 nm). However, the films sputtered at 100 W are amorphous whereas those sputtered at 120 W are crystalline with a distinct reflection from (222) plane. The present situation patent that the higher sputtering power origins the change in phase of the material, which probably indicates that the acquired more thermal energy from higher sputtering power allocates the species to diffuse over the substrate surface and occupy a proper lattice position. Further, when the thickness is compared with the structural properties, it could be perceived that the films with thickness <156 nm show amorphous structure. Having considered this low thickness, it is suspected that this could come about from the amorphous glass substrates. To authenticate this, various pieces of bare glass substrates were scanned in the 2θ ranging 10–40° and found that the obtained amorphous humps are essentially the same as shown in Fig. 2. Further, the films with thickness <156 nm were also scanned in this 2θ range and compared in Fig. 2. It is perceptible that the amorphous hump obtained from the films is very distinct from that obtained from the glass substrate. Further, the amorphous hump obtained from the ~56 nm thick films, shifts towards lower 2θ with the increasing thickness and a second hump is overlapping with the initial hump for the thickness of ~138 nm. It is now established that the obtained amorphous structure is commencing from the film itself, and the increase in sputtering power and sputtering time triggers the crystallization.

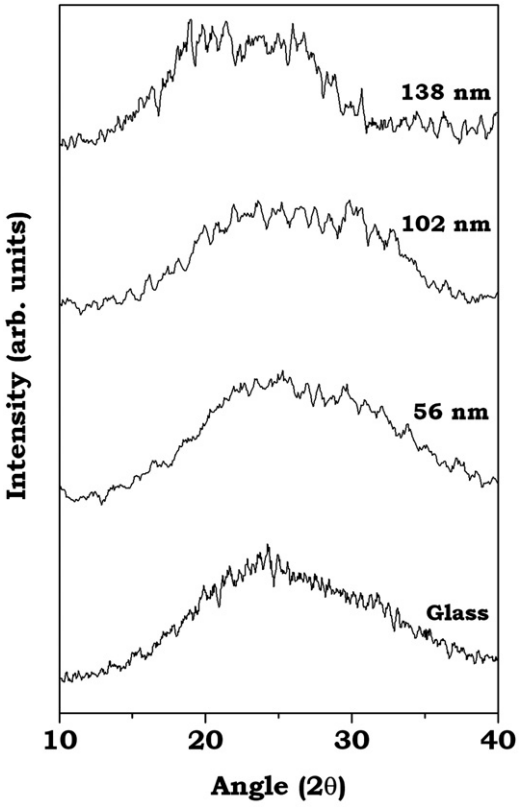

Fig. 2. Comparison of amorphous XRD patterns of IMO films with that of bare glass substrate.

3.2. Morphological studies

The surface morphologies (2D) captured from AFM is shown in Fig. 3 as a function of sputtering power ranging 40–140 W (10 min). The films were scanned on an area of 5 μm × 5 μm with a scan frequency of ~2 Hz. The surface of the films which were sputtered at 40 W contains cuboidal shaped grains with the size ranging ~60–100 nm; further, there appears an immense agglomerate of these cuboidal grains with the size of ~470 nm. This agglomerate together with the surface inhomogeneity (drain scraps and loosely packed grains) probably influences the RMS roughness to about 3.2 nm. The RMS roughness was decreased noticeably to ~2.1 nm on increasing the sputtering power to 60 W and the surface become smooth and well-packed with tiny grains together with few larger grains ranging 70–400 nm size. The RMS roughness was decreased further at 80 W to ~1.1 nm with

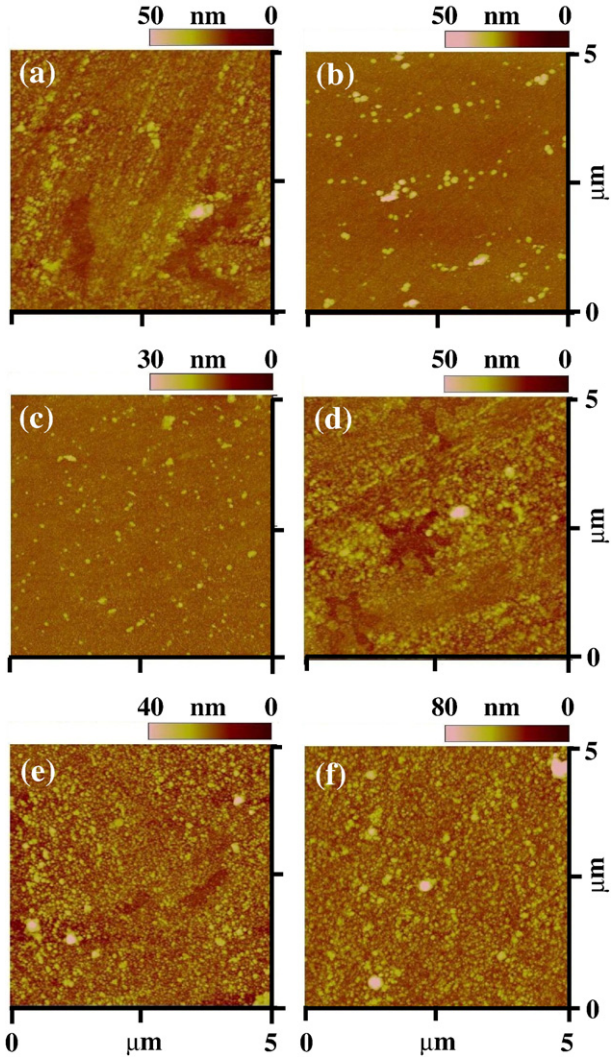

Fig. 3. AFM images (2D) of IMO films sputtered for 10 min at (a) 40 W, (b) 60 W, (c) 80 W, (d) 100 W, (e) 120 W, and (f) 140 W respectively.

smooth surface and increased number of larger grains; however the size of the larger grains decreased noticeably to the range 40–275 nm. The RMS roughness was increased considerably to ~3.8 nm at 100 W which is comprehensible as the surface contains various star-like channels on the surface with irregular and inhomogeneous grains. The RMS roughness remained the same (~3.8 nm) at 120 W whereas the channels are almost filled and the grains are more regular and homogeneous. The surface turns into rather compact and homogeneous with no presence of channels at 140 W. However the obtained maximum RMS roughness (~6.1 nm) may probably because of the colossal agglomeration of the grains (~400 nm) on the surface. The foregoing discussion propose that the RMS roughness of the films decreases with increasing sputtering power from ~3.2 to ~1.1 nm until 80 W but then increases with increasing sputter power to ~6.1 nm at 140 W.

The surface morphologies (2D) captured from AFM is shown in Fig. 4 as a function of sputtering time ranging 2.5–20.0 min (120 W). The films sputtered for minimum sputtering time of 2.5 min has an RMS roughness of ~6.1 nm; the film contains octopus-shaped channel throughout the surface which probably indicates that the nucleation and growth process is deficient; the surface contains well distinguished cuboidal shaped grains ranging 20–170 nm in size. The roughness was decreased distinctly to about 0.4 nm for the sputtering time of 5.0 min; the cuboidal shaped grains decrease in size to very tiny grains and thus decreasing the roughness; this probably suggesting that the channels are covered by subsequent nucleation and growth process. When the sputtering time is increased to 7.5 min the size of the grains again increasing in the range 30–160 nm, which probably indicates that the grains agglomerate during the subsequent nucleation process; though the surface appear compact, the roughness was increased again to ~6.6 nm which is probably due to the irregular size of grains and presence of a hole on the surface. When the sputtering time is increased to 12.5 min, the grains become highly uniform and compact with the sizes ranging from 25–80 nm and no channel left on the surface; the roughness was decreased to about 4.6 nm. The size of the grains was increased to the range of 35–

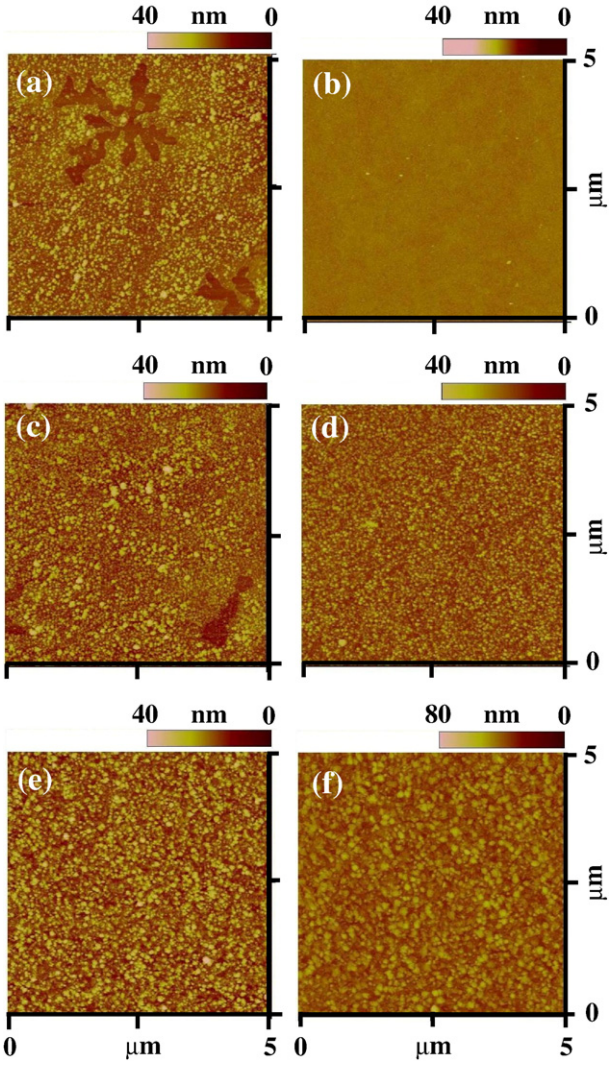

Fig. 4. AFM images (2D) of IMO films sputtered at 120 W for (a) 2.5 min, (b) 5.0 min, (c) 7.5 min, (d) 12.5 min, (e) 15.0 min, and (f) 20.0 min respectively.

120 nm on increasing the sputtering time to 15.0 min, and the roughness was decreased slightly to 4.3 nm. The size of the grains was increased further with the increasing sputtering time to reach a maximum range of 60–180 nm for 20.0 min sputtering time. The foregoing discussion concludes that the grain size and roughness are varying alternatively until 80 W which probably indicates that the nucleation and growth process are occurring simultaneously. When the sputtering time reached 12.5 min it seems like the nucleation and growth process is accomplished and the grains are increasingly agglomerating with the increasing sputtering time to reach the maximum size in the range 60–180 nm at 20.0 min sputtering time. It is now well established that the variation in sputtering power and sputtering time affects the surface morphology of the films.

3.3. Optical studies

The transmittance spectra were recorded in the wavelength ranging 300–2500 nm with a bare substrate in the path of the reference beam. Hence, the transmittance spectra refer the film transmittance alone. The average visible transmittance (AVT) in the wavelength ranging 500–800 nm was estimated and summarized in Table 1. In the case of various sputtering power (10 min), an AVT of ~81% obtained for the low sputtering power (40 W; ~57 nm thick) was increased with increasing sputtering power to a highest value of ~85% (100 W; ~157 nm thick) and then decreased to a lowest value of ~18% (180 W; ~305 nm thick) where the films turn from colorless to dark brown. This probably indicates that the oxidization of metal Mo (in the target) has reached the saturation limit due to the increased deposition rate. Further, at this sputtering power the color of the plasma was changed from bright violet to dark grayish with frequent arcing on the target surface, which probably indicated the upper limit of power density. In the case of various sputtering time (120 W), the AVT was high in the range 78–84% for the sputtering time ≤10 min, which was reduced to a range 71–76% for the sputtering time >10 min.

The optical absorption in the UV region is dominated by the optical band gap (E_g) of the semiconductor, which is related to the optical absorption coefficient (α) and the incident photon energy ($h\gamma$) as follows [7],

$$\alpha = (E_g - h\gamma)^n \quad (1)$$

where 'n' depends on the kind of optical transition that prevails. Specifically, n is 1/2, 3/2, 2 and 3 when the transition is directly allowed, directly forbidden, indirectly allowed, and indirectly forbidden, respectively. The IMO film is known to be a directly allowed semiconductor, and hence a plot is made with α^2 versus photon energy ($h\gamma$). Intersect of the x-axis from the extrapolation of the linear portion of the curve to $\alpha^2 = 0$ gives the value of E_g. The estimated values of E_g (Table 1) were varied in the range 3.75–3.90 eV, which classifies this material as wide band gap semiconductor. A maximum gap of 3.90 eV was obtained for the films sputtered at 120 W for 20 min (400 nm thick). A minimum of 3.75 eV was obtained for the films sputtered at 180 W for 10 min (300 nm thick).

Table 1 also summarizes the electrical properties estimated from the room temperature Hall measurements in Van der Pauw configuration. The negative sign of Hall coefficient confirmed the n-type conductivity of the films. As the films that were sputtered at <80 W showed high resistivity (>10^4 Ω cm), the Hall coefficients were not detectable. The maximum mobility values of 19.5 and 18.4 cm^2/Vs were obtained for the amorphous films sputtered at 80 W (for 10 min) and those sputtered for 5 min (at 120 W) with high carrier concentration values (in the order of 10^{20} cm^{-3}). Although, a minimum bulk resistivity (2.65×10^{-3} Ω cm) and a maximum carrier concentration (4.16×10^{20} cm^{-3}) were obtained for the crystalline films sputtered at 180 W (10 min), these films showed very low transmittance (AVT of ~18%) with dark brown in color. Whereas, the high AVT of amorphous films (80–90%) were decreased when the films become crystalline. This suggests that the amorphous films show better over all properties and further depositions could be carried out in order to enhance the properties of amorphous films and the effort is under progress.

4. Conclusions

Thin films of indium molybdenum oxide (IMO) were rf sputtered on glass substrates at room temperature. With the best of authors' knowledge, our group is the first to report the rf sputtering of these films at room temperature. The sputtered films were studied as a function of sputtering power (40–180 W) and sputtering time (2.5–20.0 min). It is established that the crystallization of amorphous structure occurs with the increase in sputtering power and sputtering time. It is suggested that the increase in thermal energy allocates the species to diffuse over the substrate surface and occupy proper lattice positions to become crystalline. The size of the grains and RMS roughness are found to vary with varying sputtering power and sputtering time (AFM analysis). The films possess high optical band gap in the range of 3.75–3.90 eV which classifies and promises that this material could be useful as wide band gap semiconductors in transparent electronics. The maximum mobility values of 19.5 and 18.4 cm^2/Vs were obtained for the amorphous films sputtered at 80 W (for 10 min) and 120 W (5 min) respectively, with high carrier concentration (in the order of 10^{20} cm^{-3}). Although, a minimum bulk resistivity (2.65×10^{-3} Ω cm) and a maximum carrier concentration (4.16×10^{20} cm^{-3}) were obtained for the crystalline films sputtered at 180 W (10 min), the films showed very low average visible transmittance (18%). The better over all properties conclude that the further depositions could be carried in order to enhance the properties of amorphous films and the effort is under progress.

Acknowledgements

One of the authors (E. E) thanks Portuguese Ministry of Science and Technology, and CENIMAT-I3N/CEMOP departments of New University of Lisbon, for offering postdoctoral fellowship. This work is financed by the projects CTM/38924/2001 and CTM/48853/2002.

References

[1] H. Ohta, H. Mizoguch, M. Hirano, S. Narushima, T. Kamiya, H. Hosono, Appl. Phys. Lett. 82 (2003) 823.
[2] A. Hagfeldt, M. Gratzel, Chem. Rev. 95 (1995) 49.
[3] S. Lyu, Y. Zhang, H. Ruh, H. Lee, H. Shim, E. Suh, C. Lee, Chem. Phys. Lett. 363 (2002) 134.
[4] M. Huang, S. Mao, H. Feick, H. Yan, Y. Wu, H. Kind, E. Weber, R. Russo, P. Yang, Science 292 (2001) 1897.
[5] Y. Meng, X. Yang, H. Chen, J. Shen, Y. Jiang, Z. Zhang, Z. Hua, Thin Solid Films 394 (2001) 219.
[6] E. Elangovan, A. Marques, A. Pimental, R. Martins, E. Fortunato, Mater. Res. Soc. Symp. Proc. 905E (2006) (0905-DD05-10.1).
[7] J.I. Pankove, Optical Processes in Semiconductors, Prentice-Hall, NJ, 1971, p. 34.